Cell Proliferation

Cell Prolif., 2016, **49**, 386–394 doi: 10.1111/cpr.12257

Zinc oxide nanoparticles inhibit expression of manganese superoxide dismutase *via* amplification of oxidative stress, in murine photoreceptor cells

Da Dong Guo*,#, Qin Li†,#, Hong Ying Tang‡, Jing Su§ and Hong Sheng Bi*

**Shandong Provincial Key Laboratory of Integrated Traditional Chinese and Western Medicine for Prevention and Therapy of Ocular Diseases, Key Laboratory of Integrated Traditional Chinese and Western Medicine for Prevention and Therapy of Ocular Diseases in Universities of Shandong, Eye Institute of Shandong University of Traditional Chinese Medicine, Jinan, China, †Emergency centre, Yantai Yuhuangding Hospital Affiliated Hospital of Qingdao University Medical College, Yantai, China, ‡Shandong University of Traditional Chinese Medicine, Jinan, China and §Affiliated Hospital of Shandong University of Traditional Chinese Medicine, Jinan, China*

Received 5 February 2016; revision accepted 15 March 2016

Abstract

Objectives: As a parenchymal cell, the photoreceptor is more susceptible to alterations in outer micro-environmental conditions than other cells. In the present study, we aimed to investigate inhibitory effects of zinc oxide (ZnO) nanoparticles on expression of manganese superoxide dismutase (MnSOD) in murine photoreceptor-derived cells.

Materials and methods: We investigated effects of ZnO nanoparticles on murine photoreceptor cell viability and on expression and activity of MnSOD using 3-(4,5-dimethylthiazol-2-yl)-2,5-diphenyl tetrazolium bromide (MTT) assay, immunofluorescence analysis, flow cytometry, quantitative real-time PCR and enzyme-linked immunosorbent assay (ELISA).

Results: ZnO nanoparticles were found to have higher cytotoxic effects in concentration- and time-dependent manners, to elevate intracellular levels of hydrogen peroxide and hydroxyl radicals, and thus to induce overproduction of reactive oxygen species (ROS) and collapse of mitochondrial membrane potential, leading to cell damage. Moreover, ZnO nanoparticles also significantly reduced expression of MnSOD at both the mRNA and protein levels, reduced its activity, and further aggravated oxidative stress-mediated cell damage.

Conclusion: Overall, ZnO nanoparticle-induced cytotoxicity was associated with elevated levels of oxidative stress due to overproduction of ROS and reduced expression and activity of MnSOD.

Correspondence: H. S. Bi, Professor, Eye Institute of Shandong University of Traditional Chinese Medicine, Jinan 250002, China. Tel./fax: +8653182861167; E-mail: azuresky1999@163.com

#These authors contributed equally to this work and should be regarded as co-first authors.

Introduction

Recently, zinc oxide (ZnO) nanoparticles have attracted much attention for their biomedical applications. It has been demonstrated that ZnO nanoparticles may act as a potent anti-diabetic chemical (1,2) or anti-cancer agents (3–5). However, studies have also indicated that ZnO nanoparticles possess potential genotoxicity to organisms (6–9), which is involved in the elevated reactive oxygen species (ROS) level and DNA damage. Despite making progress, the underlying mechanisms are not well understood.

Oxidative stress is caused by imbalance between ROS production and antioxidant defences, while mitochondria play an important role in ROS production and ROS scavenging (10). To protect themselves from the deleterious effect of ROS, cells have evolved many defensive mechanisms including enzymes capable of ROS removal, such as catalase, and various peroxidases for the removal of hydrogen peroxide (H_2O_2) or superoxide dismutase, eliminating superoxide radicals (11). Among these, manganese superoxide dismutase (MnSOD) is an intramitochondrial free radical scavenging enzyme in mitochondria that governs the types of ROS egression from the organelle to regulate cellular redox homoeostasis to maintain the normal mitochondrial functions (12). Therefore, MnSOD plays a key role in protecting cells, maintaining the mitochondrial integrity in cells exposed to oxidative stress and regulating cellular concentrations of ROS (13,14).

Oxidative stress can markedly enhance the generation of ROS resulting from a wide variety of stimuli and is regarded as one of the most important mechanisms

for nanomaterial-mediated toxicity (15–17). Meanwhile, the cell is equipped with myriad antioxidant enzyme systems to combat deleterious ROS production in mitochondria, with the mitochondrial antioxidant enzyme MnSOD acting as the chief ROS scavenging enzyme within the cell (18). In the present study, we aimed to investigate the effects of ZnO nanoparticles on the production of ROS and the expression of MnSOD. Our results will facilitate the understanding of ZnO nanoparticle-induced cytotoxicity and underlying mechanisms involved in the reduced MnSOD expression *via* amplification of oxidative stress.

Materials and methods

ZnO nanoparticles

The ZnO nanoparticles were purchased from Shanghai Fortunebio-tech Co., Ltd (Shanghai, China) and the purity was more than 99.7%. The appearance of ZnO nanoparticles was characterized by a field emission scanning electron microscope (SU8020; Hitachi, Tokyo, Japan), and the size distribution was measured by a Malvern Zetasizer Nano ZS (Malvern Instruments Ltd, Worcestershire, UK) with specialized software (Zetasizer Nano ZS).

Cell culture

A 661W cell line was provided by Dr Muayyad R. Al-Ubaidi (University of Oklahoma Health Sciences Center, USA). In the present study, 661W cells were maintained in Dulbecco's modified Eagle's medium (DMEM; Life technologies, Gaithersburg, MD, USA) containing 1.0 g/l of glucose, 10% foetal bovine serum (HyClone, Logan, UT, USA), 100 U/ml penicillin, 100 μg/ml streptomycin. All cells were cultured at 37 °C in water-saturated air supplemented with 5% CO_2. Cell amounts were determined with an automated cell counter (TC10; Bio-Rad, Hercules, CA, USA).

MTT assay

To determine the effect of ZnO nanoparticles on cell viability of 661W cells, MTT (3- (4,5-dimethylthiazol-2-yl)-2,5-diphenyl tetrazolium bromide) assay was performed. Briefly, 661W cells were seeded in 96-well plates (1.0×10^4 cells per well) and cultured overnight, and then treated with different concentrations of ZnO nanoparticles (dissolved with DMEM medium and dispersed by sonication prior to experiments). The final concentrations of ZnO nanoparticles were 31.25, 62.5 and 125.0 μmol/l (final volume, 200 μl per well), respectively. In the meantime, control cells were cultivated under the same conditions without addition of ZnO nanoparticles. Each culture was incubated at 37 °C for 24, 48 and 72 h in a 5% CO_2 incubator, respectively. At the indicated time, cell morphology was first observed by a bright field microscope (IX71; Olympus, Tokyo, Japan), and then cells in each well were supplemented with 20 μl of MTT solution (5 mg/ml), further cultured for another 4 h at 37 °C. After discarding the supernatant, 200 μl of dimethyl sulfoxide (DMSO) was added in each well and shaken for 10 min, then the absorbance was determined by a microplate reader (Bio-Tek ELX800, Winooski, VT, USA) at 490 nm (reference at 650 nm). Cell viability was calculated as follows: cell viability (%) = $[A]_{test}/[A]_{control} \times 100$, where A stands for relevant absorbance. Every experiment was repeated three times.

Determination of H_2O_2 and hydroxyl radical levels

ROS include superoxide, hydroxyl radical, H_2O_2, and peroxynitrite. To observe the evidence for direct actions of ZnO nanoparticles on 661W cells, in the present study, we mainly determined the changes of the levels of H_2O_2 and hydroxyl radicals by using Hydrogen Peroxide Assay Kit and Hydroxyl Radical Assay Kit (both were purchased from Nanjing Jiancheng Bioengineering Institute, China). In Brief, 661W cells were first seeded in six-well plates (5×10^5 cells per well) and cultured overnight, then the medium was discarded and cells were supplemented with 0, 31.25 62.5, 125.0 μmol/l of ZnO nanoparticles (final volume: 2 ml). Furthermore, all cells were cultured at 37 °C for another 4 h. At the indicated time, the supernatant was collected to measure the H_2O_2 and hydroxyl radical levels. The determination was strictly in accordance with the manufacturer's instructions, and every experiment was repeated three times.

Mitochondrial membrane potential ($\Delta\psi m$) analysis

To explore the effect of ZnO nanoparticles on $\Delta\psi m$ of 661W cells, measurement of $\Delta\psi m$ was performed using the lipophilic cationic probe 5,5′,6,6′-tetrachloro-1,1′,3,3′-tetraethyl benzimidazolyl carbocyanine iodide (JC-1) under various conditions. Usually, JC-1 accumulates either in the mitochondria as aggregates (whose fluorescence is red) in healthy cells or in the cytoplasm as monomers (whose fluorescence is green). During early apoptosis, the $\Delta\psi m$ collapses. As a result, JC-1 aggregates cannot accumulate within the mitochondria and dissipate into JC-1 monomers leading to loss of red fluorescence. Therefore, $\Delta\psi m$ collapse is signified by a decrease in the ratio of red to green fluorescence. In this

study, 661W cells were seeded in a six-well plate at a density of 2×10^5 cells per well and cultured overnight, then incubated with different concentrations of ZnO nanoparticles (0, 31.25, 62.5 and 125.0 μmol/l respectively) in 2 ml volume at 37 °C for 24 h. Furthermore, the cells were washed with phosphate-buffered saline (PBS) and incubated with JC-1 staining working solution (Beyotime, Haimen, China) at 37 °C for 20 min. After washing with staining buffer (Beyotime), the cells were washed with PBS, and the changes of $\Delta\psi m$ were recorded using an inverter fluorescent microscope (IX71; Olympus).

Apoptosis and/or necrosis measurement

Annexin V/PI staining can be applied to analyse the apoptosis and/or necrosis after exposure to chemicals. To evaluate the influence of various concentrations of ZnO nanoparticles on cell apoptosis/necrosis, 661W cells were seeded in a six-well plate at a density of 3×10^5 cells per well and cultured overnight, and then the cell culture medium was discarded and was supplemented with different concentrations (i.e. 0, 31.25, 62.5, 125.0 μmol/l) of ZnO nanoparticles (final volume: 2 ml), and all cells were further incubated at 37 °C in an incubator with 5% CO_2 for 24 h. In order to obtain an accurate result, both the floating and the adherent cells were collected and were washed with PBS. The cells were then resuspended using 400 μl of annexin V-FITC binding buffer (Bipec Biopharm, Cambridge, MA, USA) at a density of 1×10^6 cells/ml, followed by addition of 5 μl of annexin V-FITC. Next, samples were gently vortexed and were incubated at 4 °C in the dark for 20 min, and 10 μl of PI was further added to the cell suspension, followed by incubation at 4 °C for another 5 min in the dark. At the indicated time, all samples were immediately analysed by a flow cytometer (Accuri C6; Ann Arbor, MI, USA).

MnSOD mRNA expression

First, 661W cells were seeded in a six-well plate at a density of 5×10^5 cells/well and cultured overnight, then replaced with different concentrations (i.e. 0, 31.25, 62.0, 125.0 μmol/l) of ZnO nanoparticles (final volume: 2 ml), and further cultured for 2 h, then cells were collected and total RNA was isolated using TRIzol reagent (Invitrogen, Carlsbad, CA, USAS) according to the manufacturer's instructions prior to reverse transcription using the RevertAid reverse transcriptase (Fermentas, St Leon-Rot, Germany). Q-PCR was performed using SYBR Green Master Mix (TaKaRa, Otsu, Japan) in a Stratagene Mx3000P sequence detection system (Agilent Technologies, Santa Clara, CA, USA). The primers were designed by PREMIER 5.0 software and were synthesized by Shanghai Sangon Biological Engineering Technology and Service Company. The sequences of primers were as follows: MnSOD, forward: 5′-gtggtggagaacccaaagga-3′, reverse: 5′-gcgtgctcccacacatcaat-3′; GAPDH: forward: 5′-gaccacagtccatgacatcact-3′, reverse: 5′-tccaccaccctgttgctgtag-3′. The PCR programme was set as follows: 95 °C for 10 min, followed by 45 cycles of a 95 °C denaturation for 20 s, 56 °C annealing for 30 s and 72 °C extension for 30 s. Each sample was carried out in triplicate and the experiment was repeated for three times. The ΔΔct values were calculated as fold change in expression over 661W cells in CM ± SE after normalization to respective endogenous GAPDH control.

Determination of intracellular MnSOD protein level and the activity

The expression level of intracellular MnSOD and the activity were also determined after 661W cells were treated with different concentrations of ZnO nanoparticles. Briefly, 661W cells were seeded in a six-well plate at a density of 3×10^5 cells/well and cultured overnight, then the supernatant was discarded and supplemented with different concentrations (i.e. 0, 31.25, 62.50, 125.0 μmol/l) of ZnO nanoparticles (final volume: 2 ml). After 6 h of exposure to different concentrations of ZnO nanoparticles, the cells were harvested with 0.25% trypsin, collected by centrifugation at 4000 ***g*** for 10 min, and then the pellet was resuspended with cold PBS. After centrifugation, the cell pellet was vortexed in 0.5 ml of cold PBS, and sonicated on the ice for 15 min. After centrifugation at 5000 ***g*** for 10 min, the levels of MnSOD from cell extracts in 100 μl of the supernatant were determined by ELISA according to the manufacturer's instructions (Mouse Total SOD2/Mn-SOD DuoSet IC; R&D Systems, Minneapolis, MN, USA). Meanwhile, MnSOD activity (50 μl for each sample) was also measured using MnSOD Activity Assay Kit (Nanjing Jiancheng Bioengineering Institute, China) according to the manufacturer's instructions. The optical density was measured using a 4802S UV/Vis Double beam spectrophotometer (Unico Inc., Shanghai, China) at 550 nm, and every experiment was repeated three times.

Statistical analysis

Data were expressed as mean ± SD (standard deviation) from at least three independent experiments. One-way ANOVA was used for significant test and $P < 0.05$ is considered significant.

Results

Characterization of ZnO nanoparticles

The appearance of ZnO nanoparticles as characterized by a field emission scanning electron microscope (Fig. 1a) and the size distribution ranged from 15 to 50 nm with a mean diameter of about 30 nm (Fig. 1b).

Determination of cell viability

First, we analysed the effect of ZnO nanoparticles on the cell viability of 661W cells. Bright-field imaging illustrated that after treatment with different concentrations of ZnO nanoparticles for 72 h, the number and attachment of the ZnO nanoparticle-treated cells were both decreased compared to those of untreated cells, i.e. the higher concentrations of ZnO nanoparticles exposed to target cells, the stronger inhibitory effect on cell viability (Fig. 2a–d). Meanwhile, the results of MTT assay indicated that ZnO nanoparticles could also apparently inhibit the cell viability in time- and concentration-dependent manners (Fig. 2e).

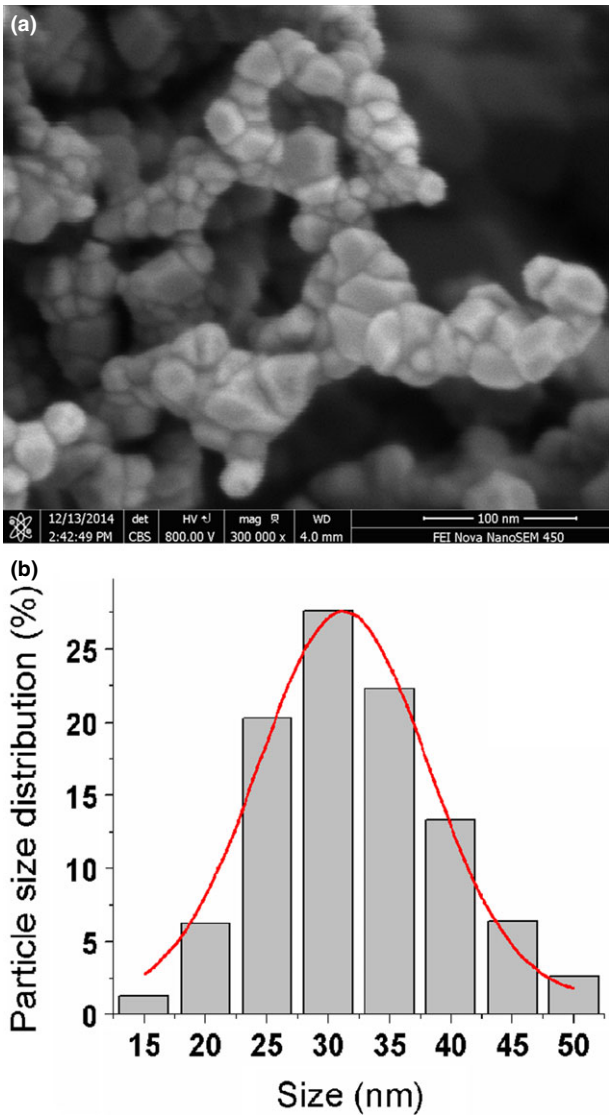

Figure 1. Image of ZnO nanoparticles characterized by a field emission scanning electron microscope (a) and the histogram of size distribution determined by a Malvern Zetasizer (b).

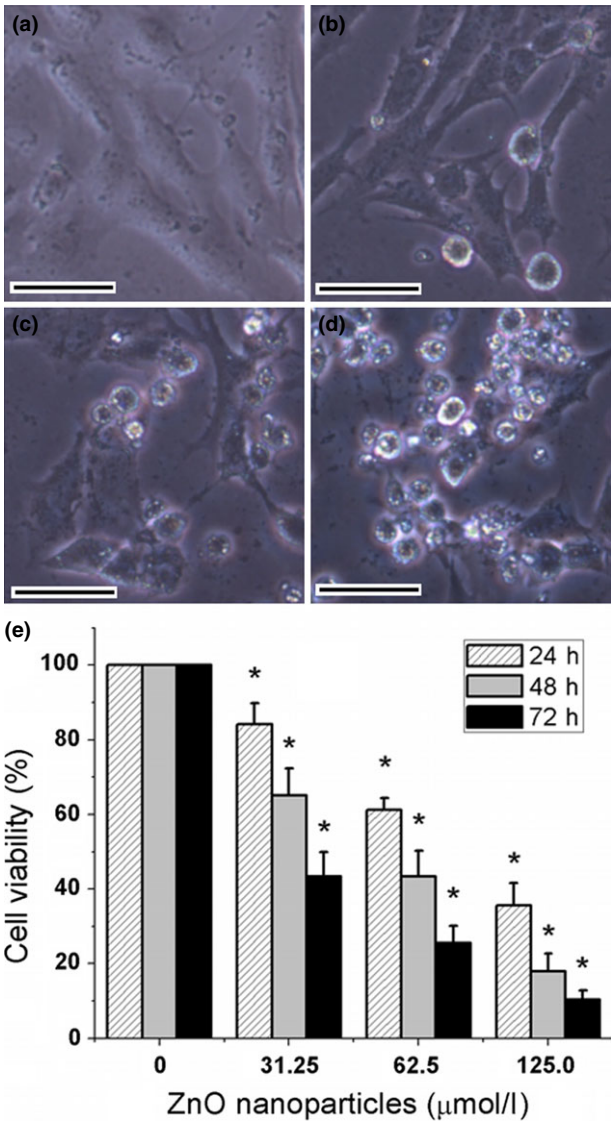

Figure 2. Typical images of murine photoreceptor cells after treatment with different concentrations of ZnO NPs for 72 h (a–d) and cell viability determined by MTT assay for 24, 48 and 72 h (e). (a) Untreated cells; (b) cells treated with 31.25 μmol/l of ZnO NPs; (c) cells treated with 62. 5 μmol/l of ZnO NPs; (d) cells treated with 125.0 μmol/l of ZnO NPs. (e) Histogram analysis of cell viability determined by MTT assay. *$P < 0.05$ versus relevant control samples, NPs = nanoparticles and bar = 20 μm.

Measurement of H_2O_2 and hydroxyl radical levels

After exposure of 661W cells to 0, 31.25, 62.5 and 125.0 μmol/l of ZnO nanoparticles for 4 h, the levels of both H_2O_2 and hydroxyl radical levels in supernatant were measured. The results indicated that the levels of H_2O_2 were significantly elevated from 68.57 ± 3.88 to 80.43 ± 4.22, 94.61 ± 6.09 and 124.88 ± 8.47 mmol/l (Fig. 3a). Similarly, the levels of hydroxyl radical were increased from 265.87 ± 20.84 to 350.30 ± 14.46, 608.33 ± 25.42 and 1174.18 ± 127.93 U/ml (Fig. 3b). These results demonstrated that with the increment of concentrations of ZnO nanoparticles exposed to 661W cells, the levels of H_2O_2 and hydroxyl radicals induced by ZnO nanoparticles were also apparently elevated, suggesting that the production of H_2O_2 and hydroxyl radicals were both in a concentration-dependent manner. Moreover, there were significant statistical differences for the amounts of H_2O_2 and hydroxyl radicals after treatment with ZnO nanoparticles compared with those of untreated cells.

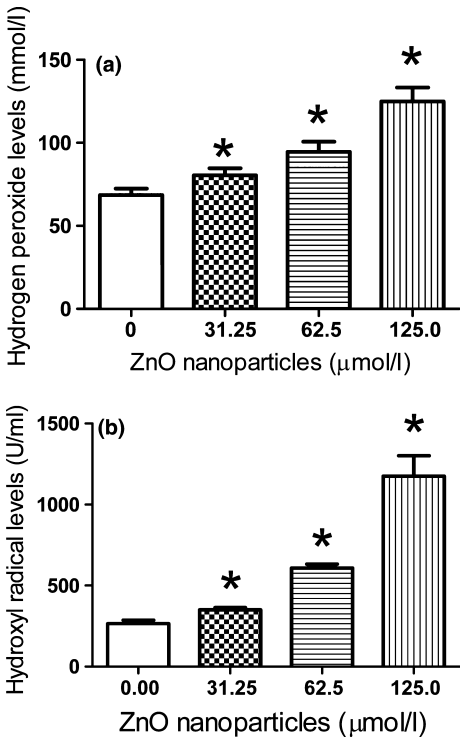

Figure 3. H2O2 and hydroxyl radical levels of murine photoreceptor cells before and after exposure to different concentrations of ZnO NPs for 4 h. (a) The alterations in H2O2 levels of murine photoreceptor cells treated with different concentrations of ZnO NPs; (**b**) the alterations in hydroxyl radical levels of murine photoreceptor cells treated with different concentrations of ZnO NPs. Significant difference was observed for both H2O2 levels and hydroxyl radical levels compared to those in untreated cells respectively. $*P < 0.05$ versus relevant control samples, and NPs = nanoparticles.

Alterations in Δψm

ZnO nanoparticles could be detected in cytoplasm after target cells exposure to these nanoparticles (6,19). To explore the influences of different concentrations of ZnO nanoparticles on 661W cells, we further analysed the Δψm alterations after target cells exposure to ZnO nanoparticles for 24 h. It was observed that the control cells possess higher Δψm (red fluorescence with high density around the cells, Fig. 4a). In contrast, Δψm of target cells was collapsed after treatment with ZnO nanoparticles (green fluorescence, Fig. 4b–d), and the intensity of green fluorescence was proportional to the concentrations of ZnO nanoparticles exposed to target cells, indicating that the Δψm collapse was significantly associated with the increment of ZnO nanoparticles exposed to cells.

Quantification of apoptosis using annexin V/PI double staining

Using double staining of annexin V-FITC and propidium iodide, live cell populations, cells entering early apoptosis and those in late-stage apoptosis/necrosis can be efficiently separated. In terms of 661W cells, a 24-h treatment made the early apoptosis rate increased from 0.8 ± 0.3% to 1.4 ± 0.4%, 3.7 ± 0.5% and 7.5 ± 0.8% respectively. Meanwhile, the level of late apoptosis/necrosis rate increased from 2.8 ± 0.4% to 10.4 ± 1.0%, 17.6 ± 2.3% and 29.8 ± 2.8% respectively (Fig. 5a–d), suggesting that longer exposure to ZnO nanoparticles markedly elevated the levels of both early apoptosis and late apoptosis/necrosis rate (Fig. 5e).

Reduction of MnSOD

The effect of different concentrations of ZnO nanoparticles on the expression level of intracellular MnSOD was investigated by Q-PCR. As shown in Fig. 6a, the level of intracellular MnSOD was decreased with the increment of ZnO nanoparticles. The mRNA levels of intracellular MnSOD were decreased to 0.384-, 0.225- and 0.076-fold after treatment with different concentrations of ZnO nanoparticles, and significant difference was observed between untreated (control) cells and ZnO nanoparticle-treated cells.

Using an ELISA technique, we determined the changes in intracellular MnSOD after 661W cells exposure to different concentrations of ZnO nanoparticles. Figure 6b indicates the decrease in expression levels of MnSOD protein with increase in concentrations of ZnO nanoparticles within 661W cells. The protein levels of intracellular MnSOD in 661W cells were decreased from

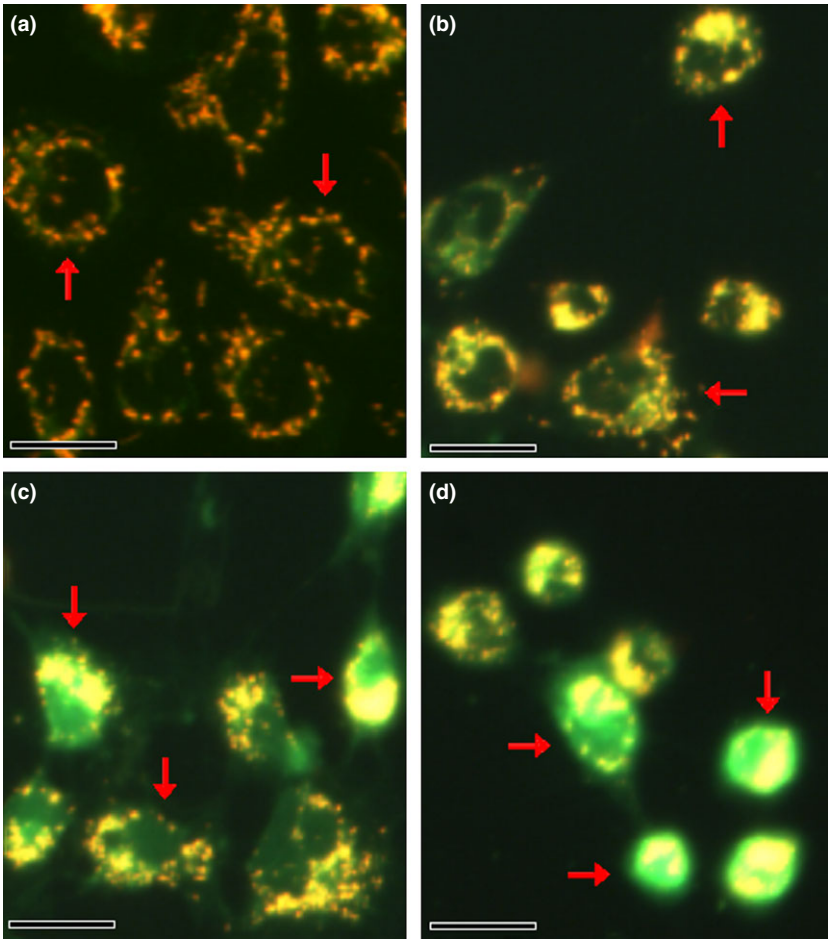

Figure 4. Typical images of Δψm in murine photoreceptor cells before and after treatment with different concentrations of ZnO NPs for 24 h. (a) Untreated cells; (b) cells treated with 31.25 μmol/l of ZnO NPs; (c) cells treated with 62.5 μmol/l of ZnO NPs; and (d) cells treated with 125.0 μmol/l of ZnO NPs. Bar = 20 μm and NPs = nanoparticles.

56.23 to 39.08, 19.11 and 12.79 ng/ml after treatment with different concentrations of ZnO nanoparticles, and accompanied by a concentration-dependent manner.

Reduction of intracellular MnSOD activity

The activity of MnSOD was also reduced after treatment with different concentrations of ZnO nanoparticles compared with that of untreated 661W cells. Figure 7 demonstrates that after treatment with various concentrations of ZnO nanoparticles, the MnSOD activity was reduced from 79.30 to 41.18, 26.48 and 15.02 U/ml, suggesting that ZnO nanoparticles could efficiently reduce the MnSOD activity.

Discussion

Investigations have shown that ZnO nanoparticles could exert cytotoxic effect on target cells, which is involved in oxidative stress (20–22). As a parenchymal cell, the photoreceptor cell line is more susceptible to the alterations in outer microenvironmental conditions than other cell lines. Therefore, we investigated the influence of ZnO nanoparticles on murine photoreceptor cell (661W) viability and MnSOD expression.

Studies have demonstrated that metal oxide nanoparticle-induced toxicity is primarily mediated by increased ROS production. Fu *et al.* found that compared to their bulk-size counterparts, engineered nanomaterials will lead to the production of higher levels of ROS and induction of oxidative damages because of their small-size, high-specific surface area and high surface reactivity (23). Our investigation showed that exposure of 661W cells to ZnO nanoparticles could cause the overproduction of H_2O_2 and hydroxyl radicals (Fig. 3). Thus, the overproduction of ROS will trigger endoplasmic reticulum stress and subsequently causes cell damage, and finally induces target cell apoptosis and/or necrosis (24).

Mitochondrial dysfunction has been proven to cause the collapse of ΔΨm, resulting in mitochondrial depolarization and release of several apoptogenic proteins into the cytosol, which may be crucial to the apoptotic pathway (25). Meanwhile, mitochondria are also major

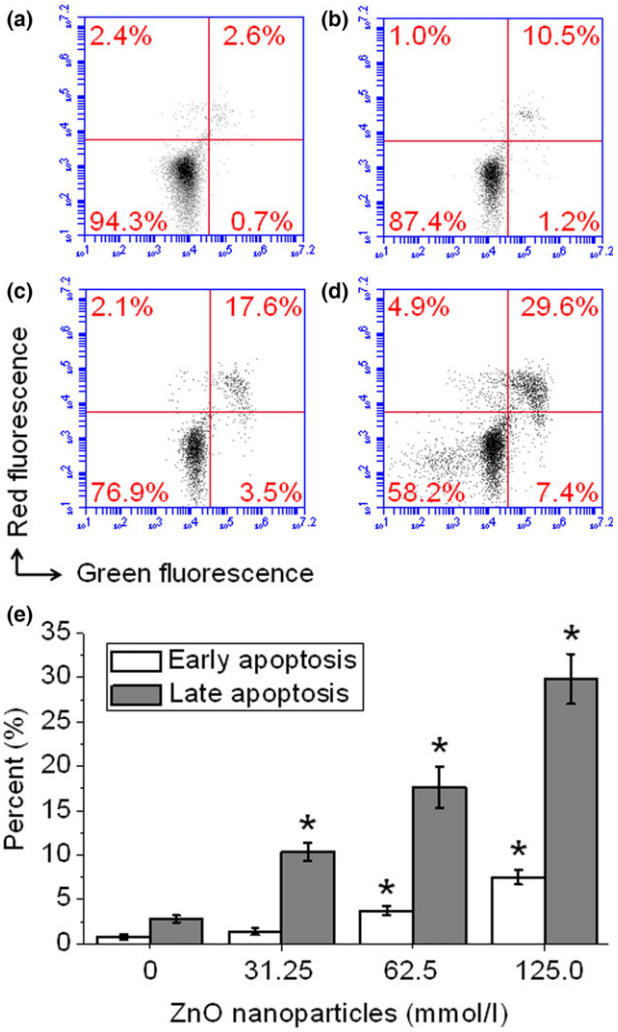

Figure 5. ZnO nanoparticle-induced cell apoptosis and/or necrosis monitored by flow cytometry. Cells were treated with 0, 31.25, 62.5 and 125.0 μmol/l of ZnO nanoparticles and cultured for 24 h, then all cells were collected, washed with cold PBS and stained with annexin V/PI double staining solution, finally all samples were determined by flow cytometry. (a) Untreated cells; (b) cells treated with 31.25 μmol/l of ZnO NPs; (c) cells treated with 62. 5 μmol/l of ZnO NPs; and (d) cells treated with 125.0 μmol/l of ZnO NPs. Measurements were repeated three times and NPs = nanoparticles. $*P < 0.05$ versus relevant control samples.

sources of ROS within the cell. Therefore, determination of both ΔΨm and ROS can provide important clues about the physiological status of the cell and the function of the mitochondria (26). In our study, we found that exposure to ZnO nanoparticles causes a collapse of ΔΨm, and the higher concentrations of ZnO nanoparticles exposed to target cells, the lower Δψm of 661W cells possessed (Fig. 4). This result indicated that ΔΨm collapse is a critical event in promoting 661W cell death after exposure to ZnO nanoparticles.

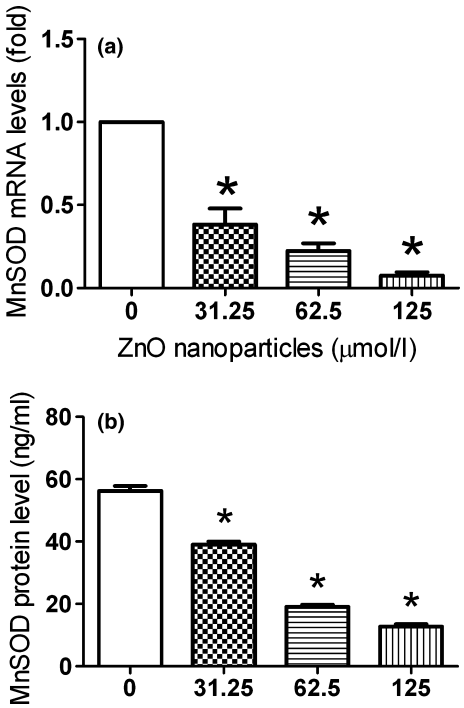

Figure 6. The expression of MnSOD at mRNA and protein levels during the ZnO nanoparticle treatment. Cells were seeded in six-well plates and cultured overnight, then treated with different concentrations of ZnO nanoparticles either for 2 h (for mRNA measurement) or for 6 h (for protein measurement). Furthermore, alterations of MnSOD in both mRNA (a) and protein (b) levels were done using quantitative real-time PCR and ELISA techniques respectively. Results were presented as mean ± SD ($n = 3$). $*P < 0.05$ versus control group.

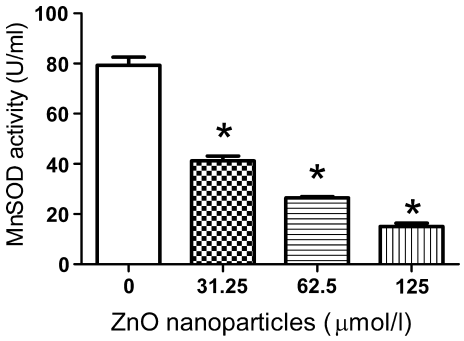

Figure 7. Determination of MnSOD activity after treatment with different concentrations of ZnO nanoparticles. Cells were treated with 0, 31.25, 62.5, 125.0 μmol/l of ZnO nanoparticles for 6 h, then every sample was collected with 0.25% trypsin, washed with PBS twice and sonicated on the ice for 15 min, centrifuged at 5000 ***g*** at 4 °C for 10 min, and then the supernatant was used to determine MnSOD activity. Data were presented as mean ± SD of $n = 3$, and $*P < 0.05$ versus control sample.

Maintenance of normal level of MnSOD in cells will be responsible for normal mitochondrial function and scavenging excessive ROS production, and then blunts

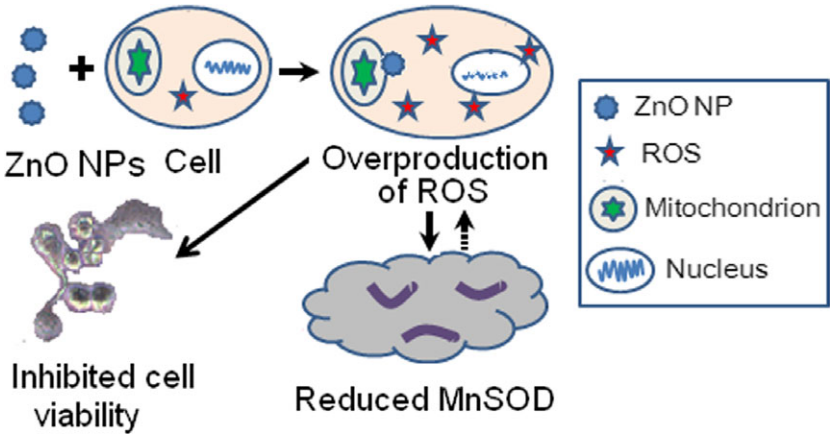

Scheme 1. Principle of ZnO nanoparticle-mediated inhibitory effect on 661W cells, which is involved in the overproduction of reactive oxygen species and reduced expression and activity of MnSOD.

the process of apoptosis (27). Our results demonstrated that cells exposed to ZnO nanoparticles will generate excessive ROS and decrease the MnSOD expression and activity. Afterwards, the decreased expression and reduced activity of MnSOD could not eliminate the excessive ROS promptly, causing accumulation of ROS within cells. Thus, accumulated ROS will further lead to cellular injury in the form of damaged DNA, lipids and proteins, finally inducing the cell apoptosis/necrosis. Shrivastava *et al.* observed that ZnO nanoparticles whose mean particle size was less than 100 nm could efficiently inhibit the expression and activity of MnSOD in whole brain, liver and blood in male mice (28), whereas Tellechea *et al.* proved that the attachment of superoxide dismutases to nanoparticles and nanostructures will not influence their activities (29). Thus, the difference of MnSOD expressions maybe varies from different organisms.

As indicated in Scheme 1, we infer that exposure to ZnO nanoparticles aggravated the overproduction of ROS, and then the high-level ROS inhibited the expression of MnSOD. Furthermore, the reduced MnSOD could not scavenge excessive ROS, which further caused accumulation of ROS and initiating the activation of related signalling pathway associated with apoptosis, finally lead to the cell damage.

Conclusions

In conclusion, the present study investigated ZnO nanoparticle-induced cytotoxic effect and underlying molecular mechanism involved in this process in murine photoreceptor cells. The results indicated that ZnO nanoparticles can apparently inhibit the cell viability in concentration- and time-dependent manners, induce cell damage via ROS overproduction and $\Delta\psi m$ collapse, and finally cause apoptosis and/or necrosis. In the meantime, the ROS overproduction can also decrease the expression of MnSOD at the both mRNA and protein levels and inhibits the activity. As a consequence, the cytotoxicity induced by ZnO nanoparticles is closely associated with ROS overproduction and the resulting oxidative stress; meanwhile, the decreased expression and activity of MnSOD mediated by oxidative stress further aggravate the cytotoxicity induced by ZnO nanoparticles on 661W cells.

Acknowledgements

This work was supported by Synergistic Innovative Center for Antivirus with Integrated Traditional Chinese and Western Medicine in Universities of Shandong Province (XTCX2014A04).

Conflict of interests

The authors declare that they have no competing interests.

References

1 Alkaladi A, Abdelazim AM, Afifi M (2014) Antidiabetic activity of zinc oxide and silver nanoparticles on streptozotocin-induced diabetic rats. *Int. J. Mol. Sci.* **15**, 2015–2023.
2 Nazarizadeh A, Asri-Rezaie S (2015) Comparative study of antidiabetic activity and oxidative stress induced by zinc oxide nanoparticles and zinc sulfate in diabetic rats. *AAPS Pharm. Sci. Tech.* [Epub ahead of print]. doi:10.1208/s12249-015-0405-y.
3 Guo D, Wu C, Jiang H, Li Q, Wang X, Chen B (2008) Synergistic cytotoxic effect of different sized ZnO nanoparticles and

daunorubicin against leukemia cancer cells under UV irradiation. *J. Photochem. Photobiol., B* **93**, 119–126.
4 Guo D, Wu C, Li X, Jiang H, Wang X, Chen B (2008) In vitro cellular uptake and cytotoxic effect of functionalized nickel nanoparticles on leukemia cancer cells. *J. Nanosci. Nanotechnol.* **8**, 2301–2307.
5 Akhtar MJ, Ahamed M, Kumar S, Khan MM, Ahmad J, Alrokayan SA (2012) Zinc oxide nanoparticles selectively induce apoptosis in human cancer cells through reactive oxygen species. *Int. J. Nanomedicine* **7**, 845–857.
6 Heim J, Felder E, Tahir MN, Kaltbeitzel A, Heinrich UR, Brochhausen C *et al.* (2015) Genotoxic effects of zinc oxide nanoparticles. *Nanoscale* **7**, 8931–8938.
7 Sharma V, Anderson D, Dhawan A (2011) Zinc oxide nanoparticles induce oxidative stress and genotoxicity in human liver cells (HepG2). *J. Biomed. Nanotechnol.* **7**, 98–99.
8 Senapati VA, Kumar A, Gupta GS, Pandey AK, Dhawan A (2015) ZnO nanoparticles induced inflammatory response and genotoxicity in human blood cells: a mechanistic approach. *Food Chem. Toxicol.* **85**, 61–70.
9 Uzar NK, Abudayyak M, Akcay N, Algun G, Özhan G (2015) Zinc oxide nanoparticles induced cyto- and genotoxicity in kidney epithelial cells. *Toxicol. Mech. Methods* **25**, 334–339.
10 Demarquoy J, Le Borgne F (2015) Crosstalk between mitochondria and peroxisomes. *World J. Biol. Chem.* **6**, 301–309.
11 Bresciani G, da Cruz IB, González-Gallego J (2015) Manganese superoxide dismutase and oxidative stress modulation. *Adv. Clin. Chem.* **68**, 87–130.
12 Hart PC, Mao M, de Abreu AL, Ansenberger-Fricano K, Ekoue DN, Ganini D *et al.* (2015) MnSOD upregulation sustains the Warburg effect via mitochondrial ROS and AMPK-dependent signalling in cancer. *Nat. Commun.* **6**, 6053.
13 Gago-Dominguez M, Jiang X, Castelao JE (2007) Lipid peroxidation, oxidative stress genes and dietary factors in breast cancer protection: a hypothesis. *Breast Cancer Res.* **9**, 201.
14 Oberley TD (2004) Mitochondria, manganese superoxide dismutase, and cancer. *Antioxid. Redox. Signal.* **6**, 483–487.
15 Guo D, Bi H, Liu B, Wu Q, Wang D, Cui Y (2013) Reactive oxygen species-induced cytotoxic effects of zinc oxide nanoparticles in rat retinal ganglion cells. *Toxicol. In Vitro* **27**, 731–738.
16 Guo D, Zhang J, Huang Z, Jiang S, Gu N (2015) Colloidal silver nanoparticles improve anti-leukemic drug efficacy via amplification of oxidative stress. *Colloids Surf. B Biointerfaces* **126**, 198–203.
17 Kung ML, Hsieh SL, Wu CC, Chu TH, Lin YC, Yeh BW *et al.* (2015) Enhanced reactive oxygen species overexpression by CuO nanoparticles in poorly differentiated hepatocellular carcinoma cells. *Nanoscale* **7**, 1820–1829.
18 Holley AK, Bakthavatchalu V, Velez-Roman JM, St Clair DK (2011) Manganese superoxide dismutase: guardian of the powerhouse. *Int. J. Mol. Sci.* **12**, 7114–7162.
19 Hackenberg S, Scherzed A, Technau A, Kessler M, Froelich K, Ginzkey C *et al.* (2011) Cytotoxic, genotoxic and pro-inflammatory effcts of zinc oxide nanoparticles in human nasal mucosa cells in vitro. *Toxicol. In Vitro* **25**, 657–663.
20 Akhtar MJ, Alhadlaq HA, Alshamsan A, Majeed Khan MA, Ahamed M (2015) Aluminum doping tunes band gap energy level as well as oxidative stress-mediated cytotoxicity of ZnO nanoparticles in MCF-7 cells. *Sci. Rep.* **5**, 13876.
21 Guan R, Kang T, Lu F, Zhang Z, Shen H, Liu M (2012) Cytotoxicity, oxidative stress, and genotoxicity in human hepatocyte and embryonic kidney cells exposed to ZnOnanoparticles. *Nanoscale Res. Lett.* **7**, 602.
22 Guo D, Bi H, Wang D, Wu Q (2013) Zinc oxide nanoparticles decrease the expression and activity of plasma membrane calcium ATPase, disrupt the intracellular calcium homeostasis in rat retinal ganglion cells. *Int. J. Biochem. Cell Biol.* **45**, 1849–1859.
23 Fu PP, Xia Q, Hwang HM, Ray PC, Yu H (2014) Mechanisms of nanotoxicity: generation of reactive oxygen species. *J. Food Drug Anal.* **22**, 64–75.
24 Guo D, Bi H, Wu Q, Wang D, Cui Y (2013) Zinc oxide nanoparticles induce rat retinal ganglion cell damage through bcl-2, caspase-9 and caspase-12 pathways. *J. Nanosci. Nanotechnol.* **13**, 3769–3777.
25 Ly JD, Grubb DR, Lawen A (2003) The mitochondrial membrane potential ($\Delta\psi$m) in apoptosis; an update. *Apoptosis* **8**, 115–128.
26 Joshi DC, Bakowska JC (2011) Determination of mitochondrial membrane potential and reactive oxygen species in live rat cortical neurons. *J. Vis. Exp.* e2704. doi: 10.3791/2704.
27 Craven PA, Phillips SL, Melhem MF, Liachenko J, DeRubertis FR (2001) Overexpression of manganese superoxide dismutase suppresses increases in collagen accumulation induced by culture of mesangial cells in high-media glucose. *Metabolism* **50**, 1043–1048.
28 Shrivastava R, Raza S, Yadav A, Kushwaha P, Flora SJ (2014) Effects of sub-acute exposure to TiO_2, ZnO and Al_2O_3 nanoparticles on oxidative stress and histological changes in mouse liver and brain. *Drug Chem. Toxicol.* **37**, 336–347.
29 Tellechea E, Cornago I, Ciaurriz P, Moran JF, Asensio AC (2012) Conjugation of active iron superoxide dismutase to nanopatterned surfaces. *IEEE Trans. Nanobioscience* **11**, 176–180.

